



**HAL**  
open science

## **How to Optimally Represent Riverbed Geometry with a Simplified Cross-Section Shape in Shallow Water Models**

Violeta Montoya-Coronado, Carole Delenne, Pascal Finaud-Guyot, Renaud Hostache

### ► **To cite this version:**

Violeta Montoya-Coronado, Carole Delenne, Pascal Finaud-Guyot, Renaud Hostache. How to Optimally Represent Riverbed Geometry with a Simplified Cross-Section Shape in Shallow Water Models. SimHydro 2021 conference : Models for complex and global water issues – Practices & expectations, Jun 2021, Sophia Antipolis, France. <10.1007/978-981-19-1600-7\_14>. <hal-03782257>

**HAL Id: hal-03782257**

**<https://hal.umontpellier.fr/hal-03782257v1>**

Submitted on 21 Sep 2022

**HAL** is a multi-disciplinary open access archive for the deposit and dissemination of scientific research documents, whether they are published or not. The documents may come from teaching and research institutions in France or abroad, or from public or private research centers.

L'archive ouverte pluridisciplinaire **HAL**, est destinée au dépôt et à la diffusion de documents scientifiques de niveau recherche, publiés ou non, émanant des établissements d'enseignement et de recherche français ou étrangers, des laboratoires publics ou privés.



HAL Authorization

# HOW TO OPTIMALLY REPRESENT RIVERBED GEOMETRY WITH A SIMPLIFIED CROSS-SECTION SHAPE IN SHALLOW WATER MODELS

Violeta A. Montoya-Coronado<sup>1</sup>, Carole Delenne<sup>2,3</sup>, Pascal Finaud-Guyot<sup>2,3</sup>, Renaud Hostache<sup>4</sup>

<sup>1</sup> Univ Lyon, INSA Lyon, DEEP, EA7429, 69621 Villeurbanne

<sup>2</sup> HydroSciencesMontpellier, Universitéde Montpellier, CNRS, IRD, Montpellier, France

<sup>3</sup> InriaLemon, CRISAM -InriaSophia Antipolis -Méditerranée, France

<sup>4</sup> Luxembourg Institute of Science and Technology, Environmental Research and Innovation Department, Esch-sur-Alzette, Luxembourg

## 1. ABSTRACT

*Riverbed geometry is crucial information of water flow models. Despite precise digital terrain models (DTM) are more widely available at rather reduced costs via RADAR or LIDAR surveys, the river bathymetry remains barely invisible. The only way to precisely measure riverbed geometry would be to carry out field surveys all along the river, which is too costly in reality. The use of physically-based models to simulate flood inundation extend is often hampered by a lack of data regarding the geometry of the riverbed. The bathymetry used is generally highly simplified and interpolated from very few measurement cross-sections. This study investigates how a river cross-section can be simplified into a trapezoidal cross-section shape, based on classically available data. The equivalent cross-section shape is defined by two parameters: the bottom elevation and the bank slope (assumed identical on both sides). The methodology is set up on a 19km length river (Alzette - Luxembourg) for which the river bed and the floodplain have been measured over 144 cross-sections. A one-dimensional hydraulic model designed using the HEC-RAS software and validated in a previous study is considered here as the reference. For each cross-section, the two parameters are calibrated, by minimising the root mean square error between the real and simplified sections. Three different cost functions are tested, based on: flow area, wet perimeter and hydraulic radius. The "real" and "simplified" hydraulic models are run under steady-state configuration with several discharge values. First results show a relatively small influence of the simplified cross-section shape on water elevation, especially for higher discharge. Next step will be to infer this optimal shape from the partial information given by the DTM.*

## 2. INTRODUCTION

Nowadays, 2D hydrodynamic modelling is frequently used for the simulation and forecasting of large-scale flood inundation. These models require topographic data to describe the river bed and floodplain geometry. Modelling large areas with structures, confluences and meanders requires a detailed description of the terrain geometry and the acquisition of in situ measurement data are time-consuming, expensive and need require data processing.

The availability of ground elevation data has increased considerably due to the recent improvements of technologies, in particular LIDAR or RADAR surveys, which provide high resolution data at a relatively low cost. However, the river bathymetry remains barely invisible for these sensors, especially the submerged surface. The lack of data regarding the geometry of the riverbed has a significant influence on numerical results. This brings to the first question: how, and on which criteria can one determine an equivalent section of the non-visible part of the river bed?

The complexity of implementing data assimilation methods with dynamic models and the difficulty of estimating the flow rate with bathymetry and roughness led to the use of simplified models derived from the de Saint-Venant, also called shallow-water equations [3]. In the last two decades the shallow water models with porosity, such as the recent depth dependant porosity approach (SW2D-DDP), appeared as a conscious way of dealing with surface hydraulic problems in the case of complex geometry [6], [7]. The geometry is roughly represented with a parameter sub-mesh (porosity) to take into account the effects of elements that are not explicitly represented in the mesh.

Furthermore, these models introduce simplification in topography and influence the line flow results in such a way that assessment of the model sensitivity is an important key step for optimizing the model performance since it can be used to define the relevant parameters for the calibration procedures [1]. This raises questions about the sensitivity of the hydrodynamic models by replacing the real topography with an "equivalent" one.

This study aims to establish an optimization method to build a cross-section equivalent to that of the real river cross-section, but with approximated geometric properties. The equivalence between the simplified and real cross-section is assessed through objective functions based on different hydraulic variables. This method is applied to the study area of the Alzette river (located north of the city of Luxembourg) to validate the model.

### 3. METHODOLOGY

#### 2.1 Equivalent cross-section shape

A “real” cross-section is generally defined by  $n$  points specifying the station  $x$  and the elevation  $z$ . It is supposed that the elevation of the left overbank can be different from the altitude of the right overbank. Water surface elevation can vary from the bottom bed to many meters above the right and left overbank. The cross-section is approximated by simpler shape based on classical available data. It is defined using two stratified geometric features where continuity of the section must be respected (see Figure 1):

- A uniform trapeze between the bottom bed ( $z_{r1}$ ) and the minimum ( $z_{r2}$ ) between the right overbank ( $z_{Rd}$ ) and the left overbank ( $z_{Rg}$ ), slope banks are the same on both sides of the trapeze,  $m$ .
- An ordinary trapeze between  $z_{Rd}$  and  $z_{Rg}$ . One of the banks is defined having the same slope as the uniform trapeze,  $m$ , and the other one is vertical slope equal to 0, so that the width of the river channel is conserved.

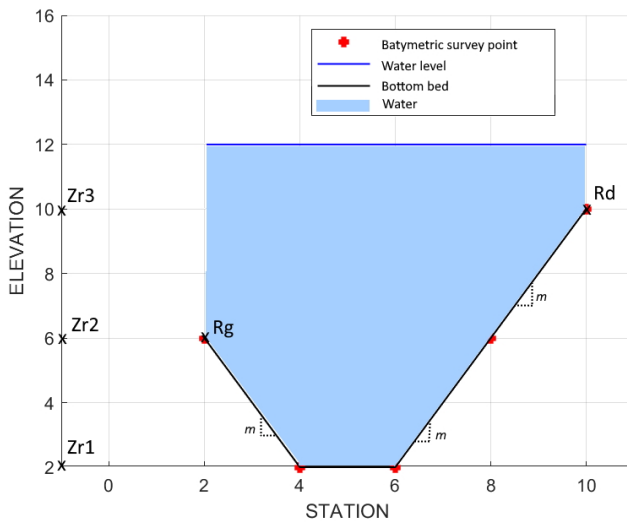


**Figure 1:** Simplified representation of a trapezoidal type section with overflow

In this simplified geometry, the bankfull width of the upper part (rectangle) depends on the river bottom width, the bank slope ( $m$ ), and the water level ( $z_s$ ). We suppose the bankfull width can be estimated from geographical data such as aerial images or digital terrain models (DTM). The water level, corresponding to the distance between water surface elevation and the bottom bed elevation ( $z_{op}$ ), is supposed to be unknown.

To recreate the simplified bathymetry one need the bank slope and the bottom bed elevations. The proposed approach therefor aims to optimize these two parameters to create a simplified cross-section with the same hydraulic properties as the real cross-section. The simplified cross-section is described with the coordinates given by equations (1) and (2).

$$x_{op} = [x_{Rg}, x_{Rg} + m(z_{Rg} - z_{op}), x_{Rd} - m(z_{Rd} - z_{op}), x_{Rd}] \tag{1}$$

$$z_{op} = [z_{Rg}, z_{op}, z_{op}, z_{Rd}] \tag{2}$$

Equations (1) and (2) give a river section physically possible only if:

- $x_{Rg} + m(z_{Rg} - z_{op}) \leq x_{Rd} - m(z_{Rd} - z_{op})$
- $z_{op} \leq z_{Rg} ; z_{Rg} \leq z_{Rd}$

A river cross-section is described by different geometry parameters (water level, bottom elevation of the riverbed, bankfull width...) and geometrical functions. Fundamental geometrical functions are: flow area  $S(z)$ , wet perimeter  $\chi(z)$  and hydraulic radius  $R_h(z)$ . These are the geometrical functions used to compare two or more sections for a specific  $z$  or an interval of  $z$ . Two cross-sections are considered equivalent when their geometric functions are equal or as close as possible for all  $z$  in a given interval.

## 2.2 Optimisation Methods: minimizing the root mean square error cost function

The objective function chosen to optimize the couple of parameters  $(m, z_{op})$  is based on the classical Root Mean Squared Error (RMSE). To simplify the optimisation process, the unnecessary root and mean are not computed and the objective function is defined as the Sum of the Squared Errors (SSE). Using the couple  $(m, z_{op})$  as parameters the process minimizes the difference between the geometric functions of the real and simplified sections. This objective function gives an SSE value; the smaller the SSE value, the smaller the difference between the two functions being compared. The SSE function needs an interval of possible  $z$  values to optimize the couple  $(m, z_{op})$  over the whole cross-section, and not only for a unique given water elevation.

It is possible to calculate the SSE with the flow area ( $SSE_S$ ), wet perimeter ( $SSE_\chi$ ), and hydraulic radius ( $SSE_{R_h}$ ). Using these geometric functions, three different optimization methods are possible. These optimization methods are described respectively in equations (3) to (5).

$$SSE_S(m, z_{op}) = \sum_{z_{inf}}^z (S_z - S_z(m, z_{op}))^2 \tag{3}$$

$$SSE_\chi(m, z_{op}) = \sum_{z_{inf}}^z (\chi_z - \chi_z(m, z_{op}))^2 \tag{4}$$

$$SSE_{R_h}(m, z_{op}) = \sum_{z_{inf}}^z (R_{h_z} - R_{h_z}(m, z_{op}))^2 \tag{5}$$

Where the interval  $[z_{inf}, z]$  is discretized in ten elements from  $z_{inf} = 2z_{r1} - z_{r3}$  to  $z = z_{r3}$ . An equivalent cross-section described by the couple  $(m, z_{op})$  is produced for each optimization method according to a different criterion. The  $SSE_S$ ,  $SSE_\chi$  and  $SSE_{R_h}$  produces three equivalent cross-sections, each of them respectively in terms of flow area, wet perimeter and hydraulic radius.

## 2.3 Validation procedure

To compare different couples of parameters obtained  $(m, z_{op})$  with each objective function ( $SSE_S$ ,  $SSE_\chi$  and  $SSE_{R_h}$ ) the relative error is used in the interval of elevation  $[z_{inf}, z]$ . It gives the dimensionless error for each altitude ( $z$ ) and allows comparison of different parameters that do not have the same dimension. To assess the influence of the cross-section simplification, the relative error is thus calculated for the flow area, wet perimeter, and hydraulic radius. Positive values are obtained when the optimized function is higher than the real one and negative values in the opposite case. The optimum case is when the relative error reaches zero.

Once the optimization method is chosen and the relative error is determined, it is necessary to check the difference in steady-state of the water line for all sections (*i.e.* the large-scale model) and the real model. The *Hec-Ras* software [8] is used for the hydraulic modelling. Two models are set up, a model with the real bathymetry and a model with a simplified bathymetry. Both models share the same forcing and parameters (left and right banks, Strickler's roughness coefficients, bridges, ...) and diverge only in the representation of the geometry of the river channel. For the 'simplified' model every cross-section is substituted by a simplified geometry defined by the left and right bank elevation, the river width and the couple of optimum parameters  $(m, z_{op})$ . Simulations are run under different steady states configurations with several discharge values. A critical depth downstream boundary condition is used for all these simulations. To cover various possible cases the model is tested with four different flows:

- Configuration 1: is a low flow such that water always remains in the river bed (no overbank flow);
- Configuration 2: is a low-medium flow such that the water overflows by 30% in half of the sections and the other half does not overflow;
- Configuration 3: is a high flow such that the water (almost) always overflows by 30% or more;
- Configuration 4: is an extreme flow such that the water always overflows by more than 80%.

## 4. RESULTS AND DISCUSSION

### 3.1 Application test case

The study reach of River Alzette is located in the Grand Duchy of Luxembourg. The reach length is approximately 19 km and the average flood plain width 300m. The basin area is about 1175 km<sup>2</sup> located between Pfaffenthal and Mersch (Figure 2). The river reach is described by 144 ground-surveyed channel cross sections whereas the floodplain topography has been extracted from a LidarDEM of 2 m pixel spacing and 15 cm vertical accuracy [4].

The method is first developed on a randomly chosen cross-section. The sensitivity of the geometric functions is assessed and one unique geometric function is set up on the 19km length of River Alzette. A one-dimensional hydraulic model designed using the HEC-RAS software and validated in a previous study [5] is also available and considered here as the reference.

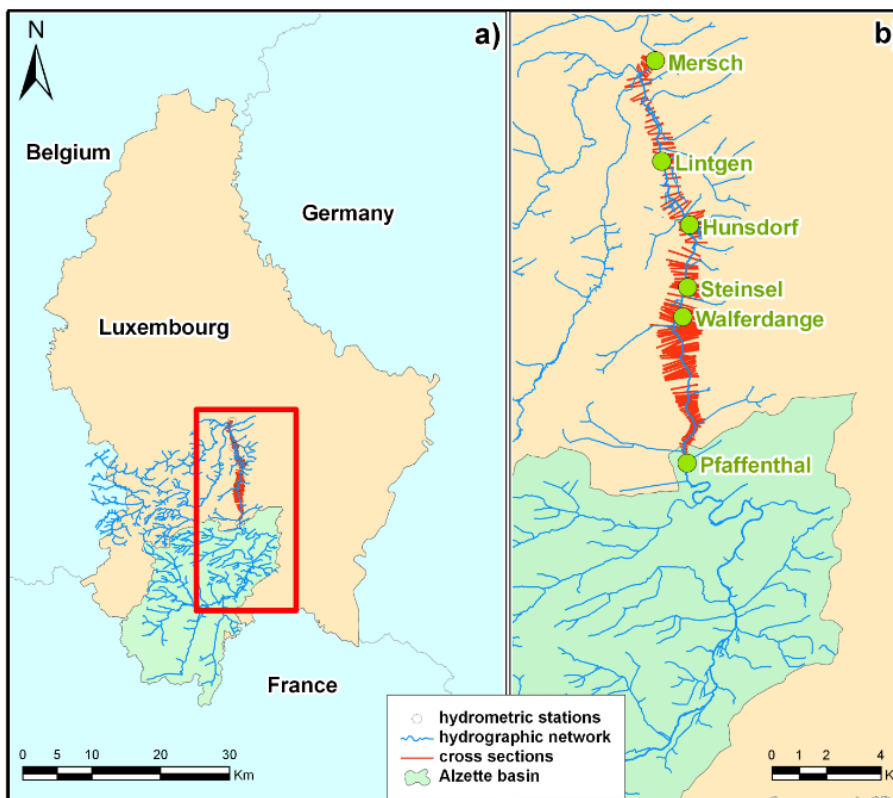


**Figure 2:** Study site in the Alzette River basin showing: (a) the drainage area down to Pfaffenthal and the 19 km river reach whose geometry is represented by the cross sections, (b) the hydrometric stations along the river (Source: [4])

### 3.2 New simplified sections

The data used in the *Hec-Ras* hydraulic model come from topographic data produced by a riverbed bathymetry survey [4] and derived from LIDAR data. Data are then used in the form of DTM and characteristics lines (description of minor bed, floodplain, dikes, ponds...). These numerical data are treated automatically and only the minor bed bathymetry is replaced by a simplified trapezoidal geometry. Optimization function is used to obtain a couple of parameters ( $m, z_{op}$ ) for each geometric function and corresponding to the minimum SSE value of the selected objective function ( $SSE_S$ ,  $SSE_\chi$  or  $SSE_{R_h}$ ).

To select the geometric function used in the hydraulic model a preliminary study is done. A typical cross-section, shown in figure 3, is selected. The flow area  $S(z)$ , wet perimeter  $\chi(z)$ , hydraulic radius  $R_h(z)$  are calculated for the water levels from 230.6 m to 239 m. Next, the SSE is calculated for every geometric functions. As said in the previous part, the couple of parameters ( $m, z_{op}$ ) is calculated by minimizing the sum of squared error with three different geometric functions:

- $SSE_S$  calculated with the flow area function
- $SSE_\chi$  calculated with the wet perimeter
- $SSE_{R_h}$  calculated with the hydraulic radius

Initial values of  $m$  and  $z_{op}$  are given in the optimization method ( $m_o, z_o$ ). For the initial value  $z_o$  the middle of the cross-section is chosen. In the case of the selected cross-section  $z_o = 234.8$  m and corresponds to the middle of the  $z$  interval: [ $z=239, z_f=230.6$ ]. Then for the initial  $m$  value we assume as initial reconstructed figure a triangle, equation (1) gives  $m_0 = \frac{x_{Rg} - x_{Rd}}{2z_0 - z_{Rd} - z_{Rd}}$  for a triangle.

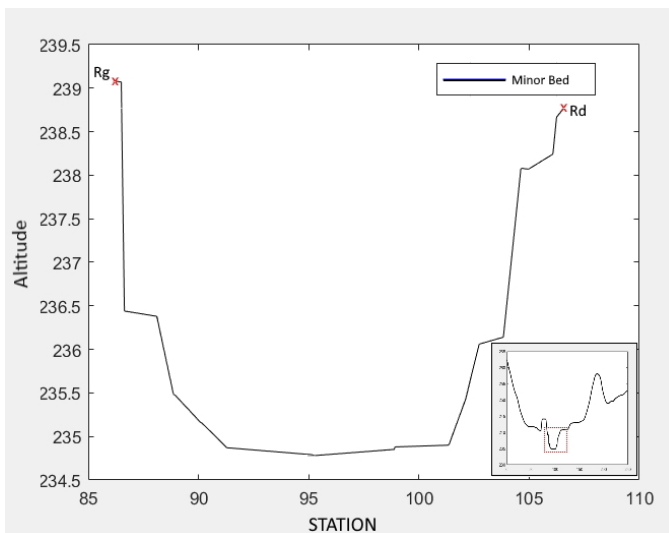


**Figure 3:** Example of Alzette’s river channel

The three optimization methods were used and three couples of parameters ( $m, z_{op}$ ) are obtained. Table 1 shows the value of optimized parameters and the SSE respective values. Numerically, for each individual cost function, the smaller the SSE the best the optimised parameters.

	$SSE_S$	$SSE_\chi$	$SSE_{R_h}$
$z_{op}$	234.9 m	234.8 m	235.8 m
$m$	0.89	0.97	2.32
SSE value	$10^{-2}$	3	64

**Table 1:** Couples of parameter ( $m, z_{op}$ ) obtained by three optimization methods :  $SSE_S$ ,  $SSE_\chi$  or  $SSE_{R_h}$  with section shown in figure 3

Three equivalent sections are recreated using the couple of values in table 1. These equivalent sections are shown in figure 4. Results shows that sections created with the  $SSE_S$  and  $SSE_{R_h}$  have a bottom bed elevation higher than the real one ( $z= 234.8$ ) whereas the bottom bed elevation of the  $SSE_\chi$  is the same as the real section figure 3. It seems that section c) figure 4 is the section giving the results further from reality due to

the difference in altitude of its bottom elevation compared to the real section. This may be the consequence of the conditions that have been made previously to obtain a realistic section:

- $x_{Rg} + m(z_{Rg} - z_{op}) \leq x_{Rd} - m(z_{Rd} - z_{op})$
- $z_{op} \leq z_{Rg} ; z_{Rg} \leq z_{Rd}$

Each optimization has been carried out using only a theoretical equation (i.e. the flow area, wet perimeter or hydraulic radius). As  $m$  and  $z_{op}$  are used to calculate other hydraulic parameters, it is also necessary to take into account the influence of each couple on all the hydraulic parameters.

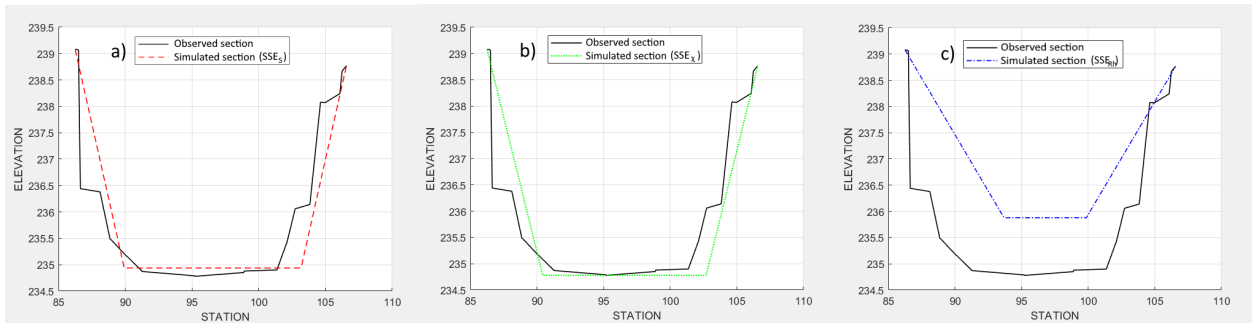


**Figure 4:** Comparison of the cross-sections of the real section and the sections recreated from (a) flow surface (b) wet perimeter, (c) hydraulic radius.

### 3.3 Comparison of optimization methods

Sensitivity analysis for couples  $(m, z_{op})$  uses the relative error comparison method. For each pair of parameters  $(m, z_{op})$  and each geometric function ( $S$ ,  $\chi$  and  $R_H$ ), the relative error curve is plotted over the interval  $z_s \in [234.8, 239]$  in figure 9. The objective is to analyse the influence of each couple on each parameter. We propose to select the optimization method enabling to minimizing the influence on the flow surface, wet perimeter, and hydraulic radius.

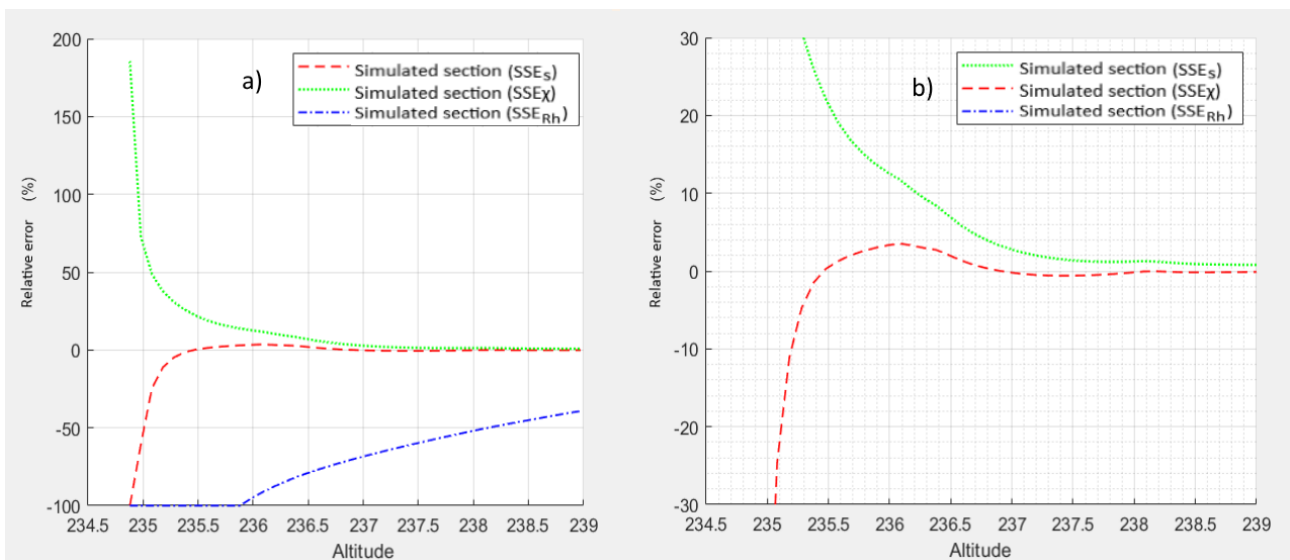


**Figure 5:** Relative error of the flow area of the sections recreated with SSEs, SSE<sub>x</sub> and SSE<sub>Rh</sub>. a) On the error interval of [-100 , 200] and b) zoomed on the error interval of [-30 , 30].

Figure 5 shows the relative error on the flow surface for all  $z_s$  in the interval  $z=239$  to  $z_{inf}=234.8$  between real section and sections created by SSE<sub>s</sub>, SSE<sub>x</sub> and SSE<sub>Rh</sub> optimization methods.

First of all, the cross-section optimized with SSE<sub>Rh</sub> underestimates the actual flow area with an error of more than 50% regardless of the  $z_s$  value. Then, the section optimized with SSE<sub>x</sub> (noted P on the figure) will overestimate the flow area from the bottom 234.8 m ( $z_{opx}$ ), up to the pre-flood elevation 239 m (left bank). However, it is from 236.25 m that the error becomes lower than 10% (the relative error is naturally high for

low  $z_s$  values for which the real section is small). For the cross-section optimized with  $SSE_s$  the real flow area is underestimated with 100% error for small values of  $z_s$ . At 235.5m the curve reaches the optimum value. And finally, from 235.5 m to 237 m there is an overestimation below 5% and finally up to river banks oscillating around the optimum value of almost zero. Section optimized with  $SSE_s$  reaches the Y-axis of 0% faster. From 235m to river banks, the error of the  $SSE_s$ -optimized section is lower than the error of the section optimized with  $SSE_\chi$ . At 239 m (the altitude before overflow), the flow area of the section recreated with  $SSE_s$  and the real section are the same, there is no over- or underestimation of the maximum volume admitted by the section. The overall result is the one expected. The section optimized with  $SSE_s$  has the lowest errors on the flow area since this section has been optimized from the flow area values from 230.6 m to 239 m.

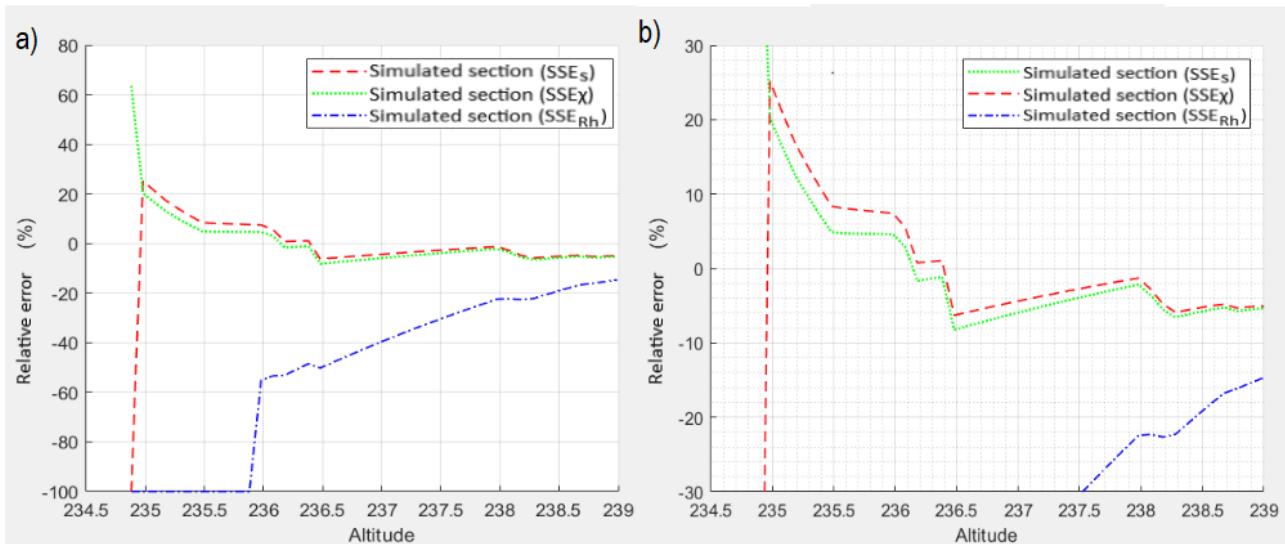


**Figure 6:** Relative error of the wet perimeter of the sections created with  $SSE_s$ ,  $SSE_\chi$  and  $SSE_{Rh}$ . a) On the error interval of  $[-100, 80]$  and b) zoom on the error interval of  $[-30, 30]$ .

As before, figure 6 shows the relative error in wet perimeter of the three simplified sections. The section optimized with the  $SSE_{Rh}$  has the largest deviation from the real section by underestimating the wetted perimeter. This is due to the altitude of  $z_{op}$  in figure 4 which is more than 1 meter above the real bottom bed altitude.

For  $z_s$  values ranging from 235 m to 236 m, the section optimized with  $SSE_s$  and  $SSE_\chi$  overestimates the wet perimeter by 20% from 235 m and up to 5% from 236 m, which can increase the energy loss and thus the pressure drop. Then, between 236 m and 236.5 m both curves reach the optimal value and then underestimate the wetted perimeter by up to 5% at the river bank altitude.

Although the section optimized with the  $SSE_\chi$  should show the smallest deviation from the real section, it can be seen at 236.25 m that the section optimized with the  $SSE_s$  shows a slightly lower percentage of error. The reason for this is that the section optimized with  $SSE_\chi$  has a  $m$  1.09 times larger than the section optimized with  $SSE_s$  and a  $z_{op}$  0.1 m deeper. At 235 m, the wet perimeter recreated with  $SSE_\chi$  is 13 m and 14 m for the section recreated with  $SSE_s$ . Considering that the real section has a perimeter of 11 m at 235m, it is the wetted perimeter recreated with  $SSE_\chi$  that will be the most adapted before the  $SSE_s$  section had the lowest error at 236.25 m because of the difference due to the smaller  $m$ .

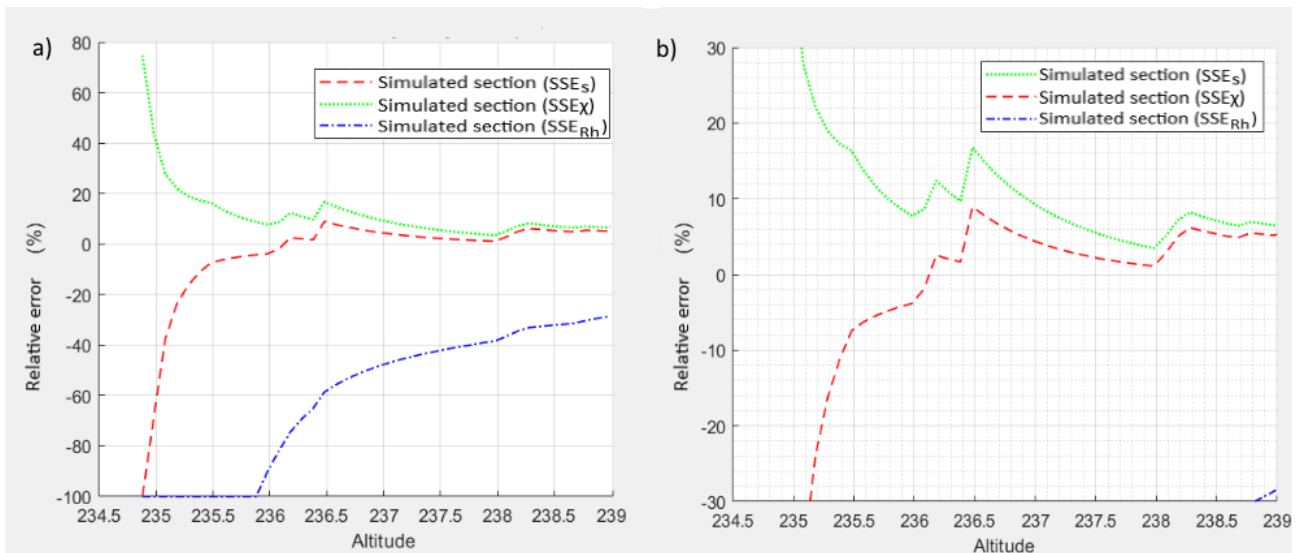


**Figure 7:** Relative error of the hydraulic radius of the sections recreated with SSE<sub>s</sub>, SSE<sub>χ</sub> and SSE<sub>Rh</sub>. a) On the error interval of [-100 , 80] and b) On the error interval of [-30 , 30].

Figure 7 shows the relative error of the three recreated sections with the optimization based on the hydraulic radius. Once again, the section optimized with the SSE<sub>Rh</sub> has very high error values with more than 30% over the whole studied interval. Then from 235 m to 236 m the section recreated with SSE<sub>s</sub> underestimates the hydraulic radius contrary to the section recreated with SSE<sub>χ</sub> that overestimates it. It is from 236.15 m that the section recreated with SSE<sub>s</sub> overestimates the actual hydraulic radius with a lower percentage of error than the section recreated with SSE<sub>χ</sub>.

Finally, the flow rate is calculated for the same section of the Alzette (Figure 3) using the Manning-Strickler equation. We assume  $S_f = S_0$  (friction slope = bottom slope),  $z = \text{constant}$  and uniform roughness. In Figure 8 the flow of the equivalent section created with SSE<sub>s</sub> seems to have the smallest deviation to the flow of the real section. This section decreases faster towards the optimum value that is reached near 235.5 m. At 239 m, the section recreated with SSE<sub>s</sub> overestimates the actual flow by 3%.

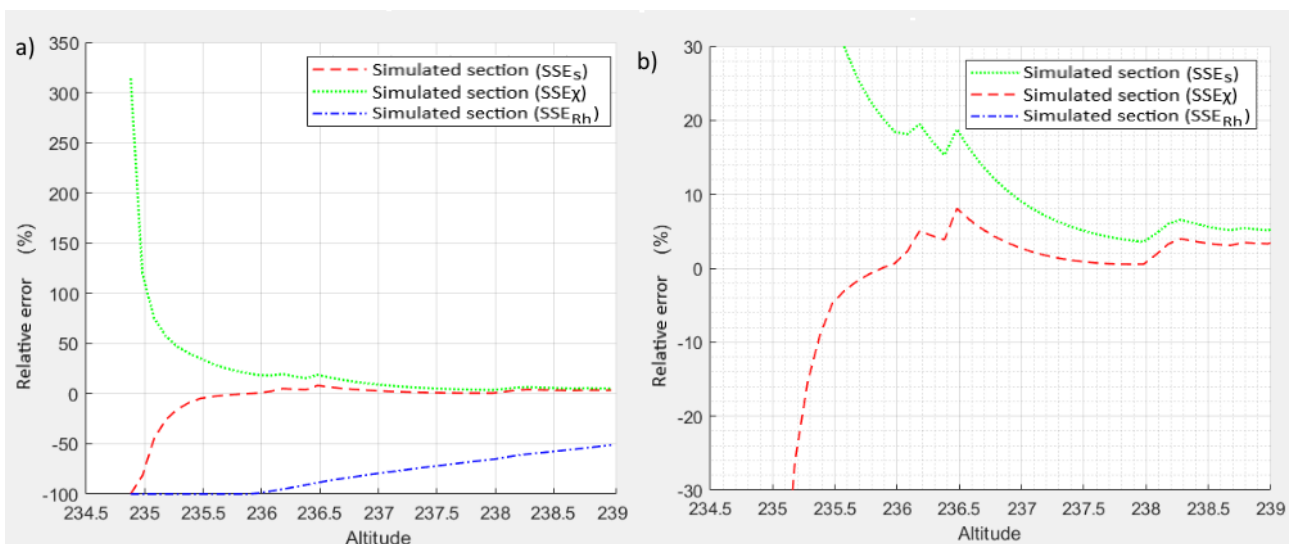


**Figure 8:** Relative error of conveyance a) the error interval of [-100 , 350] and b) zoom on the error interval of [-30,30].

Three altitudes are selected where the water level in the real section is: small ( $z_s = 235.5$  m), medium ( $z_s = 237$  m) and large ( $z_s = 238.5$  m). The error of each method for these three altitudes is compared. The analysis in Table 2 shows that for three different altitudes the SSE<sub>Rh</sub> has the highest relative error values on  $S$ ,  $\chi$ ,  $R_h$  and  $Q$  so the optimization method with the hydraulic radius equation will be rejected.

Then, the relative errors are not significantly different between the optimization with  $SSE_S$  and  $SSE_\chi$ . However, the section recreated with  $SSE_S$  has the smaller error with the exception of the point  $z_s = 235.5$  m on  $\delta\alpha_\chi$ . It is also observed at overflow ( $z_s = 238.5$  m) that the  $SSE_S$  has the smaller error percentage.

**Table 2:** Relative error of sections optimized with  $SSE_S$ ,  $SSE_\chi$  and  $SSE_{Rh}$  on  $S$ ,  $\chi$ ,  $R_h$  and  $Q$  for the altitudes 235.5 m, 237 m and 238.5 m.

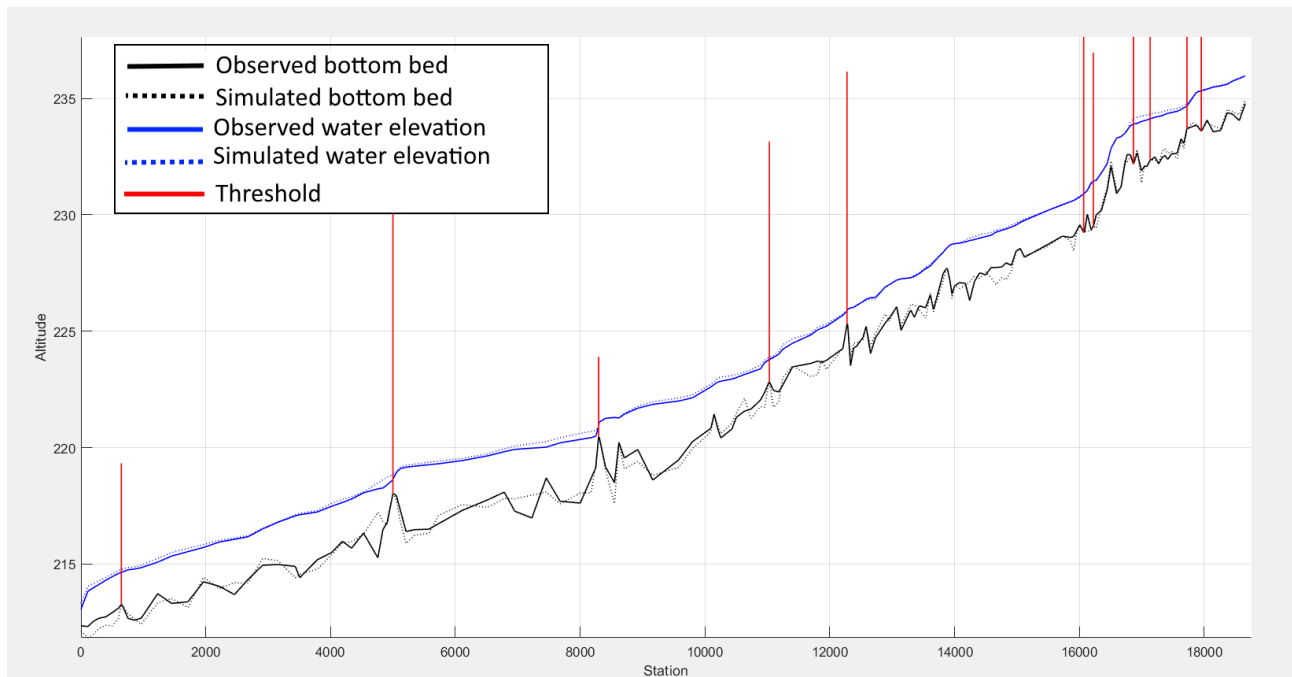
	$z_s=235.5$			$z_s=237$			$z_s=238.5$		
	$SSE_S$	$SSE_\chi$	$SSE_{Rh}$	$SSE_S$	$SSE_\chi$	$SSE_{Rh}$	$SSE_S$	$SSE_\chi$	$SSE_{Rh}$
$\delta\alpha_S$	0.1	1	-45	0.2	3	-69	0.3	2	-100
$\delta\alpha_\chi$	8	5	-100	-4	-6	-40	-5	-6	-19
$\delta\alpha_{Rh}$	-7	16	-100	4	9	-48	6	8	-32
$\delta\alpha_Q$	-5	35	-100	3	9	80	3	6	-58

Finally, as the section recreated with the  $SSE_S$  has the lowest relative errors on the three selected altitudes (Table 2), this method is set up on the 144 cross-sections along the 19km length of River Alzette.

### 3.4 Comparison of the simplified and real model under HEC-RAS

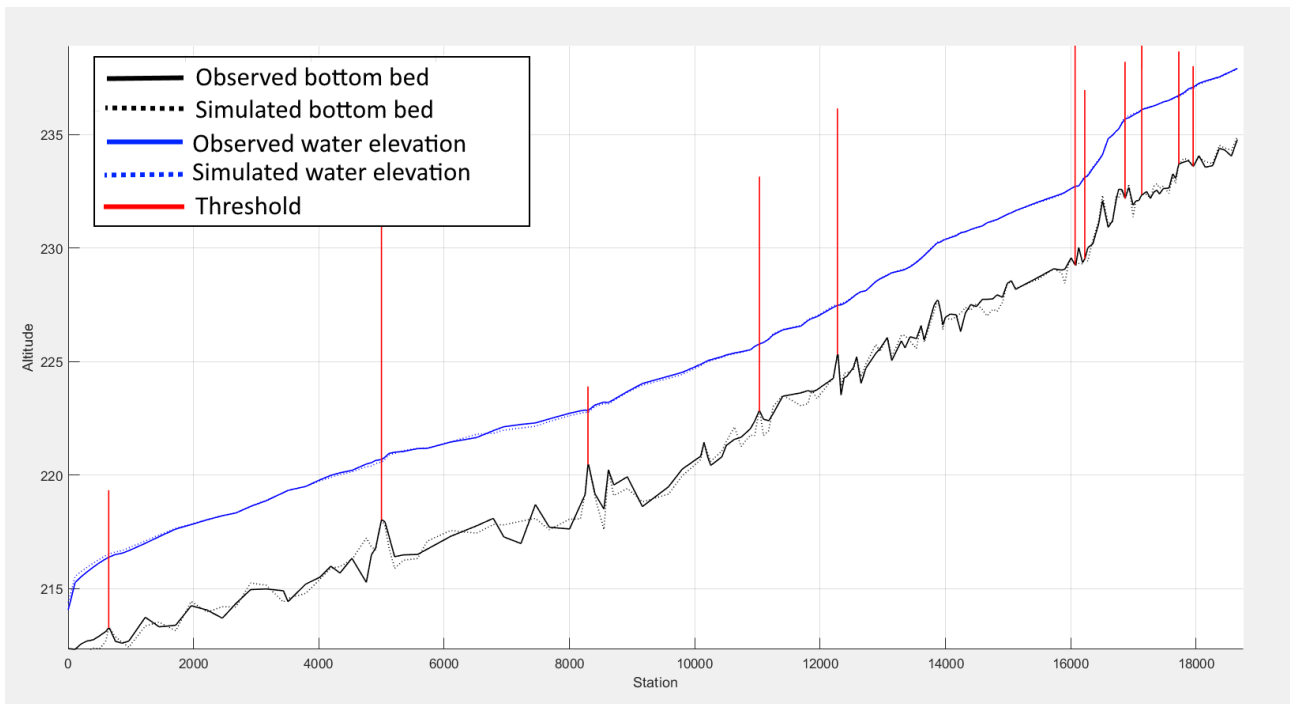
Two models of a 19 km length river (Alzette-Luxembourg) are run in steady states conditions with the *Hec-Ras* software, one with the real bathymetry [5] and the second one with the simplified bathymetry. The objective is to compare the results of the real model with the simplified model obtained by recreating each of the 144 sections with the  $SSE_S$  method. Four flow rates are selected: a small flow rate of  $10 \text{ m}^3/\text{s}$ , a low-medium flow rate of  $50 \text{ m}^3/\text{s}$ , a large flow rate of  $100 \text{ m}^3/\text{s}$  and an extreme flow rate of  $1000 \text{ m}^3/\text{s}$ . Both models will have the same information (elevation of rivers banks, Strickler coefficient, positioning of each section...) except for the positions and altitudes corresponding to the simplified part (river channel). The comparison of the models is done on water surface elevation.

Figure 9 shows the evolution of the waterline along the watercourse for a flow rate of  $10 \text{ m}^3/\text{s}$ . For this flow rate, the water remains in the river channel for all cross-sections, so that there is no overflow. The difference between the real and optimized section waterlines, show that the optimized model overestimates the water elevation by less than 0.5 m over the whole model domain.



**Figure 9:** Comparison of the water surface elevations ( $z_s$ ) and bottom elevations of the 144 sections of the Alzette flow and the 144 sections optimized for a small flow ( $10 \text{ m}^3/\text{s}$ ).

It is observed that for the 50 m<sup>3</sup>/s flow rate, in figure 10 the water level variations along the course are unstable. An underestimation of the water line of the optimized sections is observed downstream while there is an overestimation upstream. globally the greater variations c.a. 15cm are close to the weirs (represented by vertical red lines in Figures 10).



**Figure 10:** Comparison of the water surface elevations ( $z_s$ ) and bottom elevations of the 144 sections of the Alzette flow and of the 144 sections optimized for a low-medium flow (50m<sup>3</sup>/s).

With a flow rate of 100 m<sup>3</sup>/s in Figure 11, water levels of real sections are slightly higher than those of optimized sections. In cross sections with a hydraulic structure water levels fluctuate from 12-15 cm and exceptionally from 0.5 m in the 8300 m station. Between the weirs the water height difference varies from 2 to 3 cm.

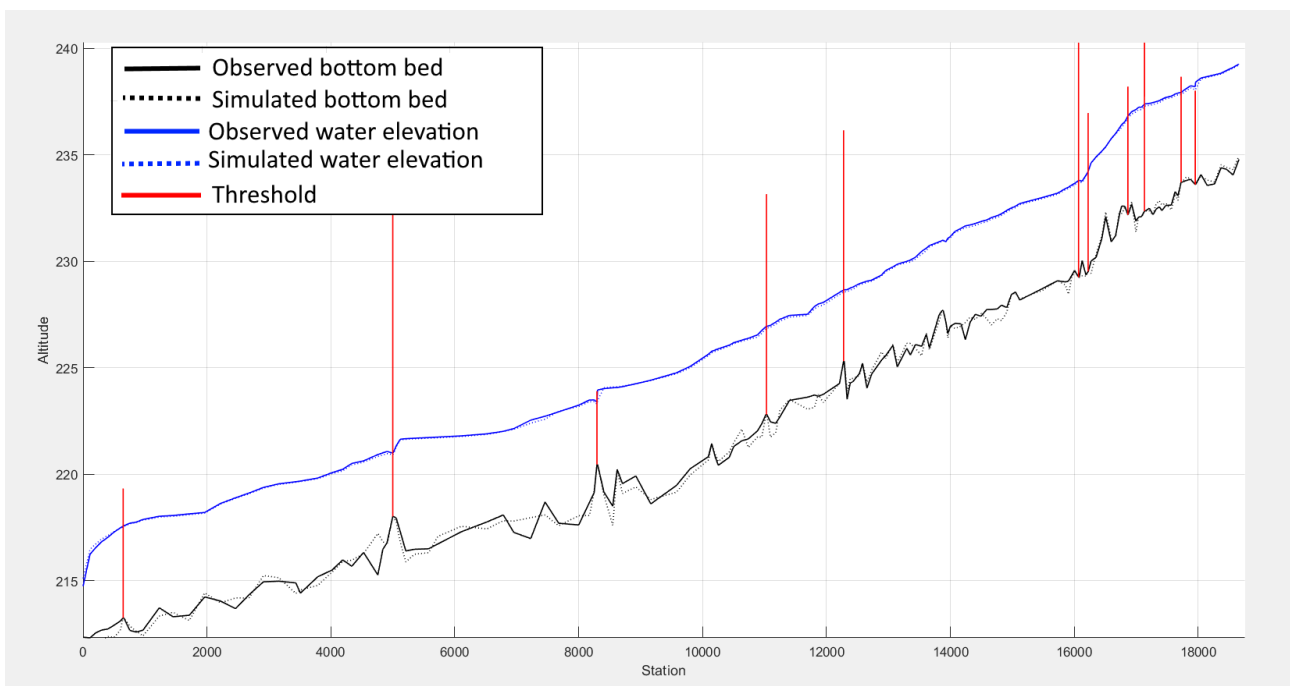


**Figure 11:** Comparison of the water surface elevations ( $z_s$ ) and bottom elevations of the 144 sections of the Alzette flow and the 144 sections optimized for a high flow rate (100m<sup>3</sup>/s).

In the last configuration (figure 12), a flow rate of  $1000 \text{ m}^3/\text{s}$  shows that water lines are quite similar with differences of a few centimetres before and after the hydraulic structures. In this case, the water volume in the channel represents only 20% of the total volume of water. This confirms that the usefulness of the optimization is not visible in this case.

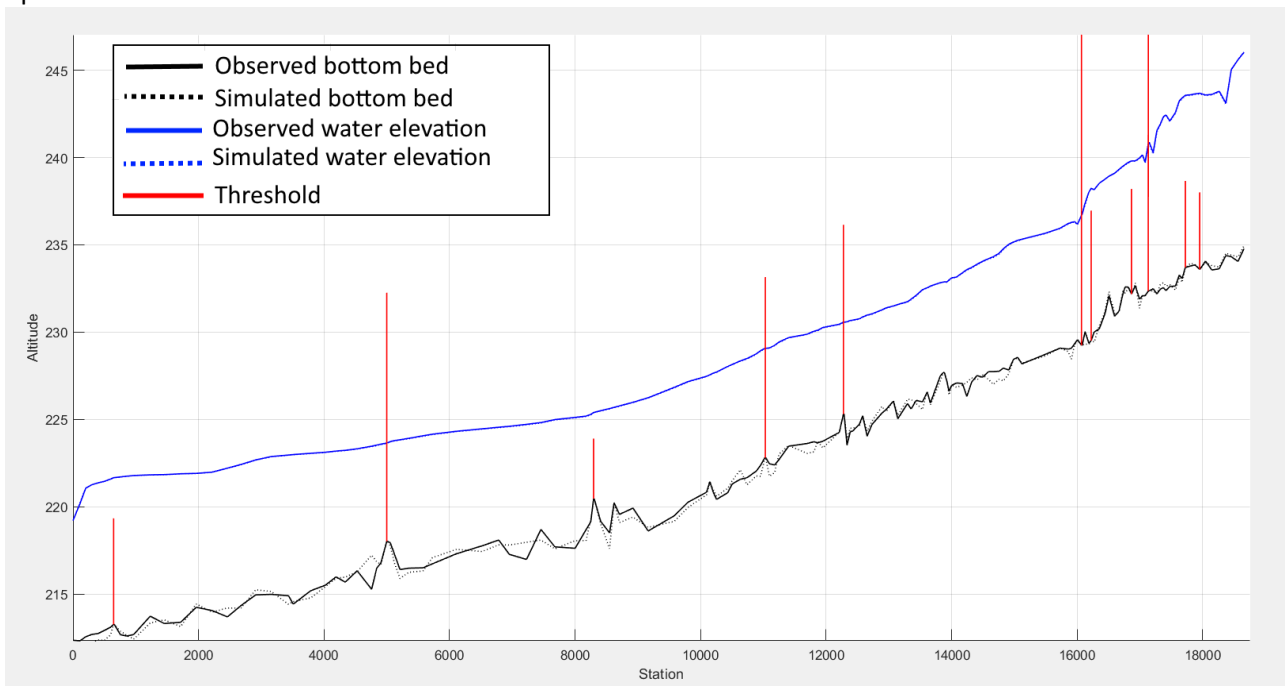


**Figure 12:** Comparison of the water surface elevations ( $z_s$ ) and bottom elevations of the 144 sections of the Alzette flow and the 144 sections optimised for an extreme flow ( $1000\text{m}^3/\text{s}$ ).

To conclude this sensitivity analysis of the model to different flow rates scenarios shows that for some sections the real water levels are over-estimated and underestimated for low flow rates, especially near the weirs. However, the difference between water levels in the real and simplified model is negligible for extreme flows.

## 5. CONCLUSIONS

In order to estimate an equivalent riverbed bathymetry, we evaluated an optimization procedure based on various geometric functions of the flow surface, wet perimeter and hydraulic radius. An optimization method has been therefore defined making use of the sum of the squares of the deviations as an objective function.

Simplifying the riverbed shape on a 19 km long reach of the Alzette river shows that it is possible to optimize a section from complete observations. The optimization method based on the flow surface yields the smallest deviation from the real section on the various parameters. However, it is important to bear in mind that this conclusion was drawn based on a single section.

A complete *Hec-Ras* model was used on 19 km of the Alzette river in order to study the consequences of this optimization on the waterline. This comparison indicates that for a small flow (no overflow) and medium flow (with some sections overflowing) the difference in water levels are of a few centimetres (c.a. 3 cm) far from the weirs and higher near the weirs (c.a. 15 cm). For extreme flows, the method used for the optimization of the simplified bathymetry does not significantly influence the waterline.

Next steps will be to apply the methodology with partial observations (i.e. with a more restricted  $z$  interval). The sensitivity of the model should be studied with partial observations as input data, and then a parameter correction algorithm should be proposed to reduce, as far as necessary, the resulting error.

## 6. REFERENCES AND CITATIONS

- [1] C. Delenne, P. Finaud-Guyot, V. Guinot, and B. Cappelaere (2011) Sensitivity of the 1D shallow water equations with source terms: Solution method for discontinuous flows. *International Journal for Numerical Methods in Fluids*, 67 :981-1003.
- [2] G. Schumann, P. Matgen, L. Hohmann, R. Hostache, F. Pappenberger, and L. Pfister (2007) Deriving distributed roughness values from satellite radar data for flood inundation modelling. *Journal of Hydrology*, 344 :96-111.
- [3] Hind Oubanas, Igor Gejadze, Pierre-Olivier Malaterre, and Franck Mercier (2018) River discharge estimation from synthetic swot-type observations using variational data assimilation and the full saint-venant hydraulic model. *Journal of Hydrology*, 559 :638-647.
- [4] R. Hostache, P. Matgen, L. Giustarini, F.N. Teferle, C. Tailliez, J.-F. Ihy, and G. Corato (2015) A drifting gps buoy for retrieving effective riverbed bathymetry. *Journal of Hydrology*, 520 :397-406.
- [5] R. Hostache, P. Matgen, G. Schumann, C. Puech, L. Hoffmann and L. Pfister, "Water Level Estimation and Reduction of Hydraulic Model Calibration Uncertainties Using Satellite SAR Images of Floods," in *IEEE Transactions on Geoscience and Remote Sensing*, vol. 47, no. 2, pp. 431-441, Feb. 2009, doi: 10.1109/TGRS.2008.2008718.
- [6] Vincent Guinot (2017) A critical assessment of flux and source term closures in shallow water models with porosity for urban flood simulations. *Advances in Water Resources*, 109 :133-157.
- [7] V. Guinot, C. Delenne, A. Rousseau, & O. Boutron (2018). Flux closures and source term models for shallow water models with depth-dependent integral porosity. *Advances in Water Resources* 109, 133-157.
- [8] US Army Corps of Engineers, Hydrologic Engineering Center (2006). HEC-RAS, River Analysis System User's Manual.